

Studies into a high performance composite connection for high-rise buildings

G.B. Lou¹ and A.J. Wang^{*2}

¹ State Key Laboratory for Disaster Reduction in Civil Engineering, Tongji University, Shanghai, P.R. China

² Corporate Technical Management, CapitaLand Management (China) Co., Ltd., Shanghai, P.R. China

(Received June 30, 2013, Revised July 27, 2014, Accepted February 27, 2015)

Abstract. This paper presents experimental and numerical studies into the structural behavior of a high performance corbel type composite connection adopted in Raffles City of Hangzhou, China. Physical tests under both monotonic and quasi-static cyclic loads were conducted to investigate the load carrying capacities and deformation characteristics of this new type of composite connection. A variety of structural responses are examined in detail, including load-deformation characteristics, the development of sectional direct and shear strains, and the history of cumulative plastic deformation and energy. A three-dimensional finite element model built up with solid elements was also proposed for the verification against test results. The studies demonstrate the high rigidity, strength and rotation capacities of the corbel type composite connections, and give detailed structural understanding for engineering design and practice. Structural engineers are encouraged to adopt the proposed corbel type composite connections in mega high-rise buildings to achieve an economical and buildable and architectural friendly engineering solution.

Keywords: composite structures; physical test; composite connection; high-rise building; finite element modelling

1. Introduction

The Raffles City Project is located in the central business district of Hang Zhou, China. The project is composed of two 60 storey 250 m tall super high-rise twisting towers and a commercial podium and 3 storey basement car parking. The overall construction floor area of the project is approximately 390,000 m². Composite moment frame plus concrete core structural system is adopted for the tower structures. Concrete filled steel tubular (CFT) columns together with steel beams reinforced concrete (SRC) beams form the outer moment frame of the tower structures. The internal slabs and floor beams are of reinforced concrete. Fig. 1(a) shows the artistic image of the project, while the structural system of the towers is shown in Fig. 1(b).

The structural design of the composite connection between CFT columns and SRC beams need to safeguard the overall structural stability through the fully rigid connections and avoid scarifying any tailored space in the meantime. The conventional ring beam type composite connection is regarded to be bulky and not suitable because of its inference with the façade erection and interior

*Corresponding author, Ph.D., E-mail: aaron.juan.wang@gmail.com

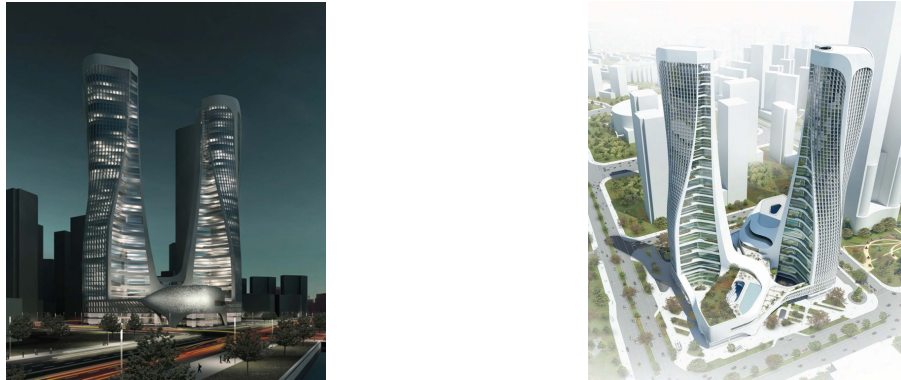
decoration. An innovative and high performance corbel type composite connection is proposed with a minimum intrusion into the interior space to achieve the fully rigid connection. Fig. 2 presents geometrical configurations for both types of connections.

This paper presents both experimental and numerical studies into the structural behavior of this high performance corbel type composite connection. Physical tests under both monotonic and quasi-static cyclic loads were conducted to investigate the load carrying capacities and deformation characteristics this new type of composite connection. A three-dimensional finite element model was also proposed and carefully calibrated. The studies give detailed structural understanding for engineering design and practice.

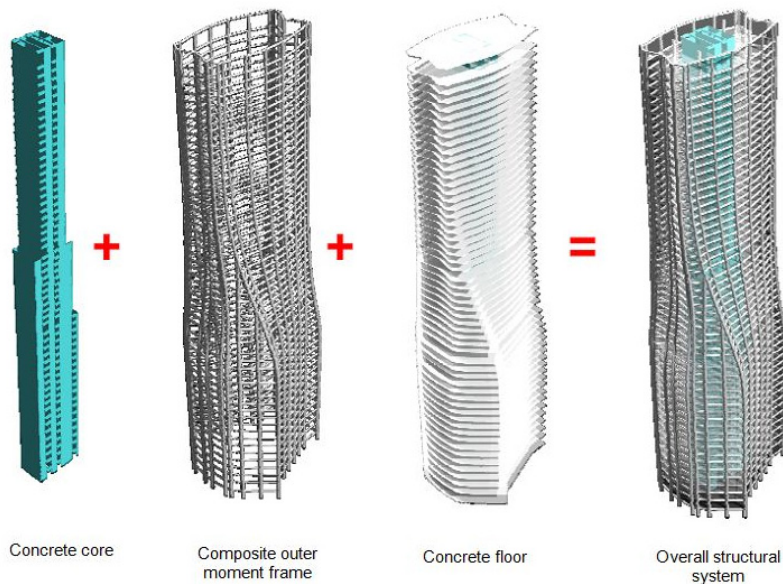
2. Literature review

According to Eurocode 4: Part 1.1 (BSI 2004), the design of both rotational stiffnesses and moment capacities of composite beam-column joints are based on the relevant clauses in Eurocode 3: Part 1.8 (BSI 2005) for steel joints with the incorporation of the contribution of tensile reinforcement. Other codes of practice with similar design philosophy are also available (AISC 2005, Brockenbrough and Merritt 2006, SCI & BCSCA 2002, Lawson and Gibbon 1995). According to these codes of practice, different components of composite beam-column joints are to be analyzed and designed separately for different failure locations. By summing up the load carrying capacities and the stiffnesses of these components with the consideration of their associated lever arms, the moment capacities and the rotational stiffnesses of the composite beam-column joints can be obtained. However, none of the design codes gives guidance regarding the rotational capacities of composite joints and they should be determined according to physical tests. (BSI 2004).

A large number of physical tests on different types of composite end-plate and fin-plate joints with various cross-sectional configurations and joint details were conducted in the past two decades (Davison *et al.* 1990, Li *et al.* 1996, Brown and Anderson 2001, Xiao *et al.* 1994, Fang *et al.* 2000). Composite joints with both composite slabs and solid slabs were investigated under either gravity or lateral loads. Full shear connection was provided in all these joint tests. Based on the results of these tests, different failure modes at various components and locations of the composite end-plate joints were identified. Empirical and semi-empirical design rules were formulated to predict the load carrying capacities and the stiffnesses of various components of the composite end-plate joints under various loading conditions. Finite element models using beam-column elements were proposed by Xiao *et al.* (1994), Nethercot and Li (1995) and Queiroz *et al.* (2005) to study the structural behaviour of composite frames. The effects of semi-rigid joints were also incorporated into the models, in which the moment-rotation curves of the semi-rigid joints were obtained from tests on various composite joints or relevant design rules. With the carefully selected stress-strain curves for both reinforced concrete flanges and steel beams, it was demonstrated that these finite element models were able to predict the structural behaviour of the composite frames conservatively. Due to the geometrical complexity of the various types of the composite joints and the limitation on the test data, the moment-rotation curves could only be defined on a case-by-case base and were quite difficult to be normalized. In addition, the scale of the physical tests is normally limited by the capacity of the loading cells. Thus, it is necessary to propose a three-dimensional finite element model to predict the stiffness and load carrying capacities of composite joints with practical geometrical configurations as an extension of physical tests.



(a) Artistic image



(b) Tower structural system

Fig. 1 Raffles City Hangzhou, China

Vasdravellis *et al.* (2009a) conducted both numerical and experimental studies into the behavior of exterior partial-strength composite beam-to-column connections. Physical tests and numerical analyses were carried out to study the seismic behavior of semi-rigid partial-strength steel-concrete composite beam-to-column joints. The specimens exhibited large dissipative capacities and very stable and ductile behavior without significant reduction in strength and stiffness. Further studies were also conducted on the dynamic response of composite frames under various degrees of shear connectors (Vasdravellis *et al.* 2009b). One-story one-bay moment-resisting frames with steel-concrete composite beams were tested under base acceleration on the shaking table. Experimental results demonstrated that for different degrees of partial interaction between the slab and the beam the response of the specimens varied significantly.

A three-dimensional finite element model was proposed by Ahmed and Nethercot (1996) to

assess the effects of shear and axial forces on the load carrying capacities of composite end-plate joints. Shell elements were used to model the steel beams, and the steel columns as well as the end-plates. Initial imperfection was also incorporated to capture any possible local buckling. Beam-column elements were used for the simulation of both the tensile reinforcement and the shear connectors. The cross-sectional areas of the beam-column elements were taken as the cross-section areas of the tensile reinforcement as well as those of the shear connectors. The concrete flanges were modelled with beam-column elements, and the doweling effects due to physical contact between the shear connectors and the surrounding concrete was not modelled properly, leading to errors in the prediction of the load-slippage characteristics of the shear connectors. Wang (2010) proposes a three dimensional finite element model and a simplified two-dimensional finite element model to study the nonlinear structural behaviour of composite end-plate connections under gravity loads. Solid elements were adopted to simulate the concrete slabs and steel beams, while the nonlinear spring elements were adopted to model the bolts and shear connectors. After calibration with test data, it was demonstrated that both numerical models are able to simulate reasonably the structural behaviour of composite joints under gravity loads. The three-dimensional finite element model was extended by Wang (2011) to study the structural behaviour of end-plate composite connections under combined gravity and lateral loads. The two-dimensional finite element model was later extended to study the structural behaviour of semi-continuous composite beams with various levels of boundary condition and connection ductility (Wang 2012). Both models were verified to be able to provide a better understanding of the structural behaviour of the end-plate semi-rigid composite connections in multi-storey moment frame buildings.

All of the above-mentioned studies are mainly on semi-rigid composite connections through either end-plates or fin-plates. With the booming in the construction industry in Asia in the past decades, more and more mega high-rise composite buildings are being developed, which require a high level of connection rigidity and ductility to ensure the overall building stability and safety under extreme loads. Thus, it is highly desirable to study the high performance composite joints with a higher level of rigidity, strength and ductility to suit the current trend in the construction industry.

3. Connection configuration

The proposed corbel type composite joints include the following key components as shown in Figs. 2(b) and 3:

- *The corbel and ring stiffener as butt welded to the CFT column:*

In order to ensure a full strength rigid connection, the I-section corbel is enlarged and stiffened together with a ring stiffener as welded inside the steel tube, so that the overall rigidity and load carrying capacity of the connection is not less than that of a typical SRC beam section.

- *The tapered section from the corbel to the steel beam:*

In order to ensure a smooth loading and stress transfer from the corbel in the joint region to the ordinary SRC beam, a tapered steel section is proposed with a slope of 1:6.

- *The steel section in the SRC beam:*

The ordinary I-steel section in the composite SRC beam is fully connected to the outer edge of

the corbel through full bolted joints on both flanges and webs.

- *Lapped reinforcement bars:*

All the longitudinal reinforcements are lapped around the flanges of the steel corbel, so that both the loads and stress can be transferred from the longitudinal main reinforcements onto the corbel in the connection region.

- *Concrete encasement*

All above mentioned components are encased with C35 concrete to ensure a composite action.

In order to achieve a full strength connection between the SRC beam and CFT column, the corbel together with the ring stiffener is strengthened to the strength and rigidity of an ordinary SRC beam. Thus, satisfactory deformation and plastic energy absorbing capacities can be achieved with a preferred failure mode and location of the plastic hinge.

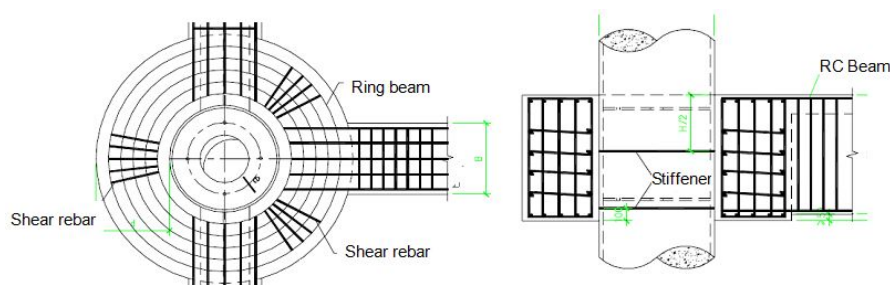
4. Objectives and scope of work

This paper presents experimental and numerical studies into the structural behavior of the high performance corbel type composite connection. Through the physical tests under both monotonic and quasi-static cyclic loads, the load carrying capacities and deformation characteristics are studied carefully. A finite element model is also proposed for the verification of the experimental results. The scope of work of the research study includes the follows:

- Experimental investigation including 2 monotonic tests and 2 quasi-static cyclic tests;
- Establishment and calibration of a finite element model for the verification of the experimental results; and
- A detailed examination of the test and numerical results revealing detailed structural understanding for engineering design and practice.

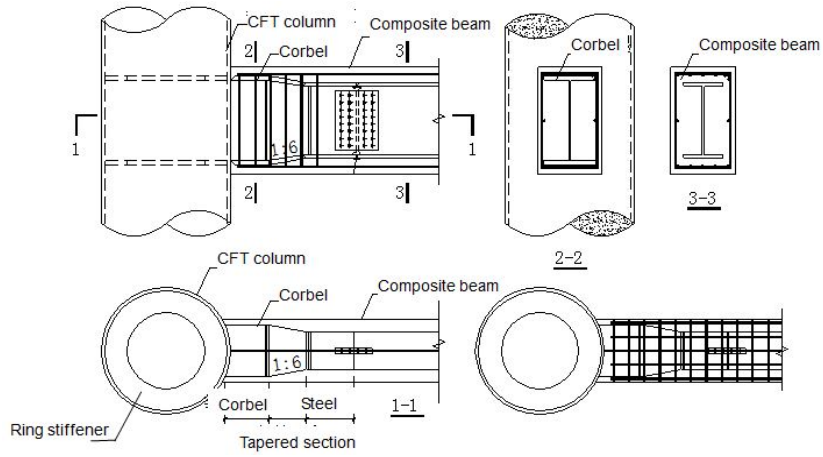
Particular attention is also given to the following aspects through the studies:

- Load carrying capacity and stress distribution;
- Load-deformation characteristics and connection energy absorption capacities; and
- Typical failure modes.



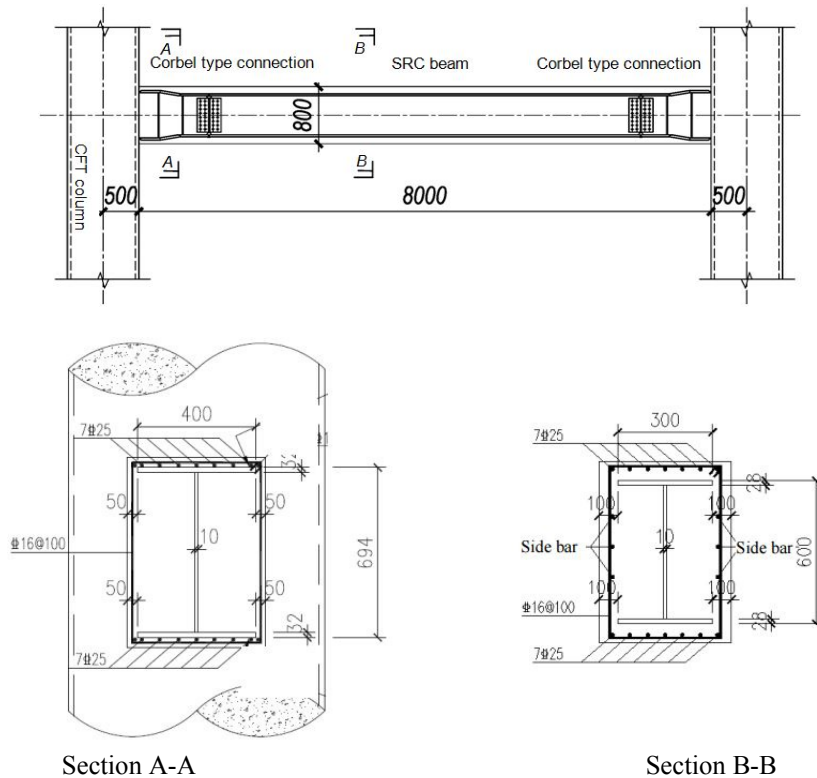
(a) Conventional ring beam type connection

Fig. 2 Composite connections



(b) Corbel type composite connection

Fig. 2 Continued



*Note: Ring stiffeners of 200 mm wide and 30 mm thick are welded inside the steel tubular column at the top and bottom flanges of the corbel.

Fig. 3 Outer frame of Raffles City Towers

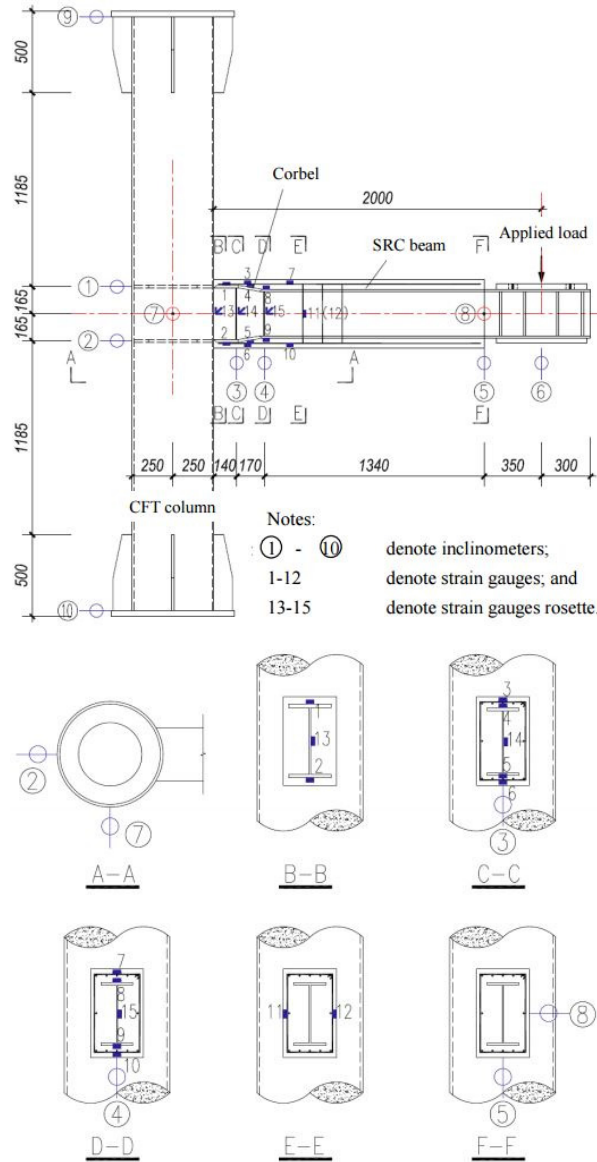


Fig. 5 Arrangement of instrumentation

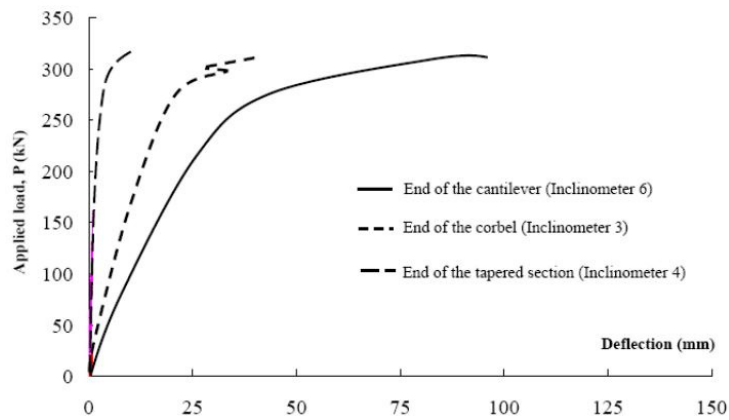
Table 1 Material properties of steel

		Thickness, <i>t</i> (mm)	Yield strength, <i>f_y</i> (N/mm ²)	Ultimate strength, <i>f_u</i> (N/mm ²)	Elongation limit, δ (%)	<i>f_u</i> / <i>f_y</i>
Beam and corbel	Web	6	354.7	505.1	33.3	1.42
	Top flange	14	386.0	533.3	34.7	1.38
	Bottom flange	16	365.8	540.9	34.7	1.48
Column	Steel tube	16	390.4	504.1	31.3	1.29

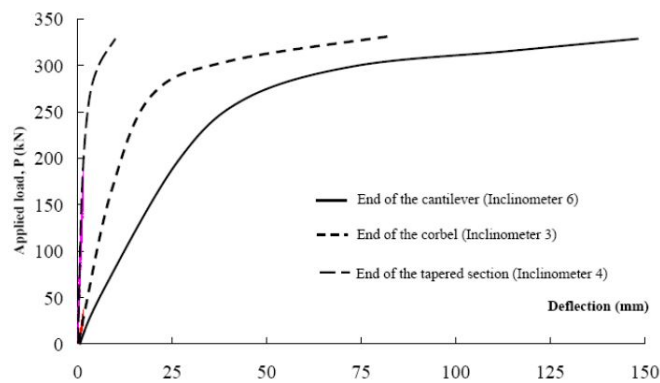
thickness of all steel webs, flanges and stiffeners is also scaled down accordingly. As shown in Fig. 5, various instrumentations are carefully arranged on the specimen to capture accurately the structural response throughout the tests as shown in Fig. 5. The dimensions of the specimens are indicated in Figs. 3 and 4, while Table 1 presents the measured material properties of the steel sections.

C60 concrete is adopted for the column, while the concrete grade of the beam is C35. A total of 4 specimens are tested. Specimens SP1 and SP2 are tested under monotonic loading and SP3 and SP4 under quasi-static cyclic loading.

For the monotonic loading tests, each load step is initially set to be 5% of the estimated overall load carrying capacity, and refined to 2.5% near the failure of the specimen. A pre-load of 15% of the estimated load carrying capacity is applied in order to ensure a directly hard contact of the loading cell and the specimen. For quasi-static cyclic loading tests, the displacement control approach is adopted with the applied displacement of $\pm\Delta_y/2$, $\pm\Delta_y$, $\pm2\Delta_y$, $\pm3\Delta_y$, $\pm4\Delta_y$, $\pm6\Delta_y$, where Δ_y is the displacement at the first yield of the steel connection. The loading protocol ensures a suitable preloading and sufficient applied displacements to test the overall ductility of the composite connection in the meantime. The test methods and procedures stated in CABR (1997) and ASTM (2011) are also considered.



(a) Specimen SP1



(b) Specimen SP2

Fig. 6 Load-deflection curves

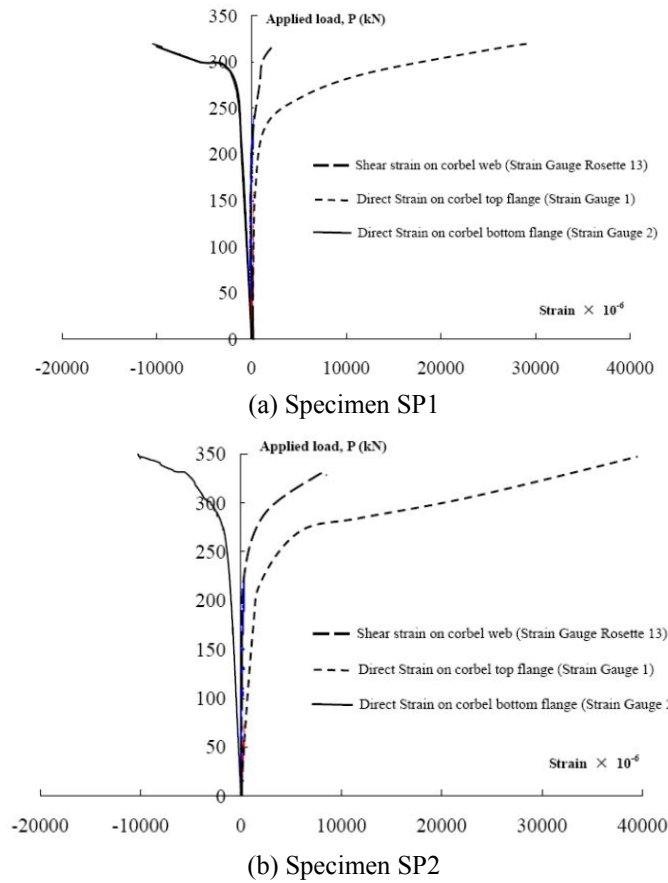


Fig. 7 Load-strain curves

6. Test results

6.1 Specimens under monotonic loads (Specimens SP1 and SP2)

Figs. 6-7 present the results of the monotonic tests on Specimens SP1 and SP2, while Fig. 8 presents a typical failure mode. It is noted that the load carrying capacities of both specimens are tested up to 321.0 kN and 332.1 kN respectively, and their cantilever end deflections at failure are 30.6 and 25.6 mm respectively.

A close observation on the strain development also shows that the direct tensile strain at the top flange is 30 to 50% higher than the compressive strain of the bottom flanges due to the contribution of the concrete material. It is noted that the shear strain in the web is significantly smaller than the strain in the flange, which is just above the yield strain. This is preferred for a high-rise building in a seismic sensitive region like Hangzhou, where the Project located.

Cracking is first observed in the tensile region near the tapered location of the connection at the applied load of 200 kN. Cracks further propagate to the neutral axis of the section near failure. Concrete crushing is observed in the compressive region of the connection at an applied load up to 300 kN. Obvious deformation is observed at the tapered section directly outside the corbel

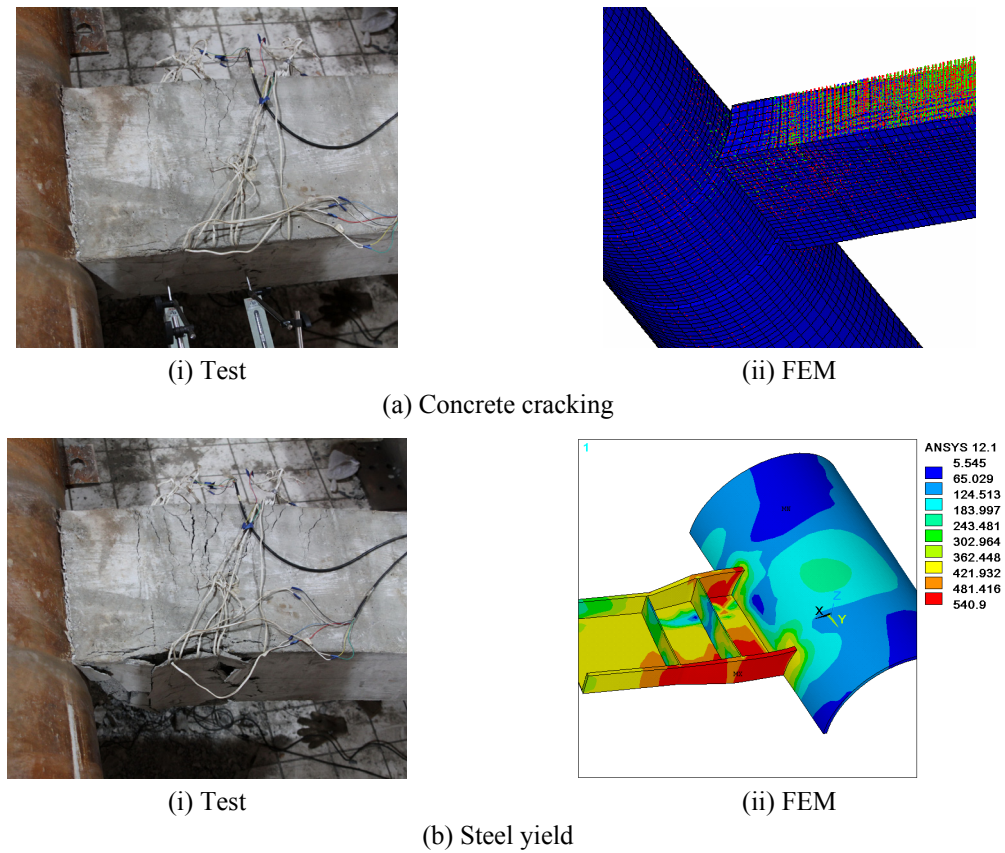


Fig. 8 Typical failure mode

connection region, which is regarded to be the weakest location of the specimen. This also demonstrates the connection region in itself is strong and rigid enough to undertake the bending moments and shear forces from the ordinary beam section. Meanwhile, the overall deflection of the cantilever at failure is around 4 times of that at the first yield, and high deformation capacities and ductility are observed in both Specimens SP1 and SP2. Due to the relatively high strength and stiffness of the CFT column, the overall structural integrity is still maintained at the inner ring stiffener and the column even at the failure of the composite connection.

In order to assess the rigidity of the composite connections, the load-deflection characteristics of the composite connections are also transferred into normalized moment-rotation curves according to Eurocode 3, Part 1.8 (BSI 2005). The normalized applied bending moment, m , is defined as

$$m = \frac{M}{M_{bp}} \quad (1)$$

where M is the applied bending moment to the connection; and M_{bp} is the moment capacities of the SRC beam.

The normalized rotation can be calculated as follows

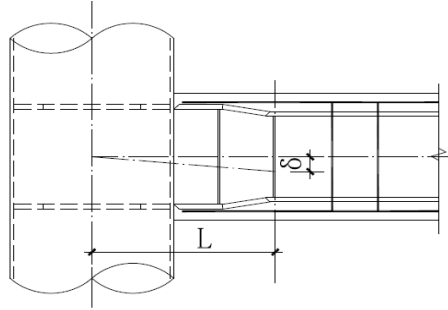
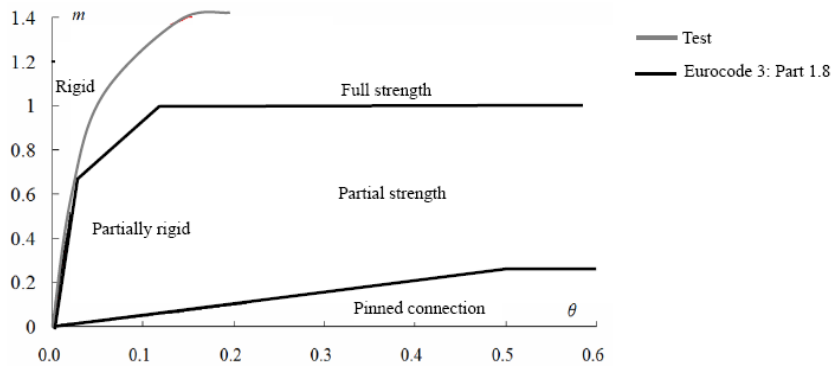
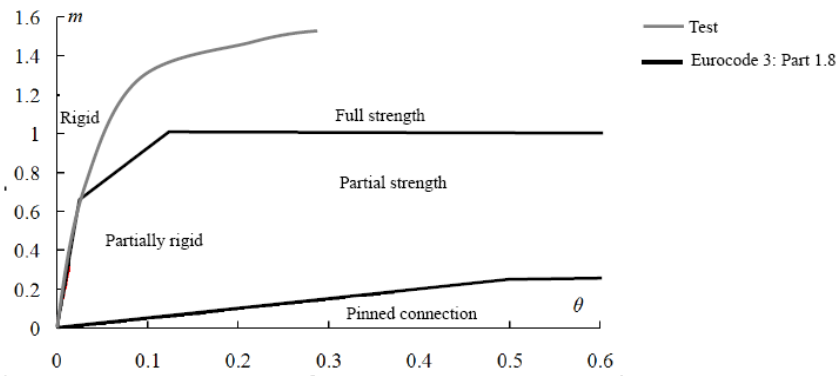


Fig. 9 Definition of connection rotation



(a) Specimen 1



(b) Specimen 2

*Note: Refer to Section 6.1 for the definitions of the normalized applied bending moment, m , and the normalized connection rotation, θ

Fig. 10 Normalized moment-rotation curves

$$\theta = \frac{\theta_r}{M_{bp}} \frac{EI_b}{L_b} \quad (2)$$

where EI_b is the sectional bending stiffness of the SRC beam;

L_b is the span of the SRC beam; and
 θ_r is the rotation of the connection and equal to δ/L as defined in Fig. 9.

The normalized moment-rotation curves as also compared with those defined in Eurocode 3, Part 1.8 (BSI 2005) for pinned and fully rigid connections as shown in Fig. 10. It is observed that both full rigidity and full strength can be achieved through the proposed corbel type composite connection, which is well aligning with the structural design philosophy of the Project.

6.2 Specimens under quasi-static cyclic loads (Specimens SP3 and SP4)

The quasi-static cyclic loading tests were conducted on both Specimens SP3 and SP4. The first yield displacement at the end of the cantilever is observed at about 30 mm, as seen from the results of the monotonic loading tests in Fig. 6. Figs. 11 and 12 present the load-deflection and moment-rotation curves of Specimens SP3 and SP4. It is noted that the maximum applied load is up to 320 kN, and the applied loads are able to be maintained at the level of 300 kN after multiple loading circles without apparent unloading or pre-mature knock down. The maximum deflection is up to 4 times of the first yield deformation of the composite connection, which exhibits relatively

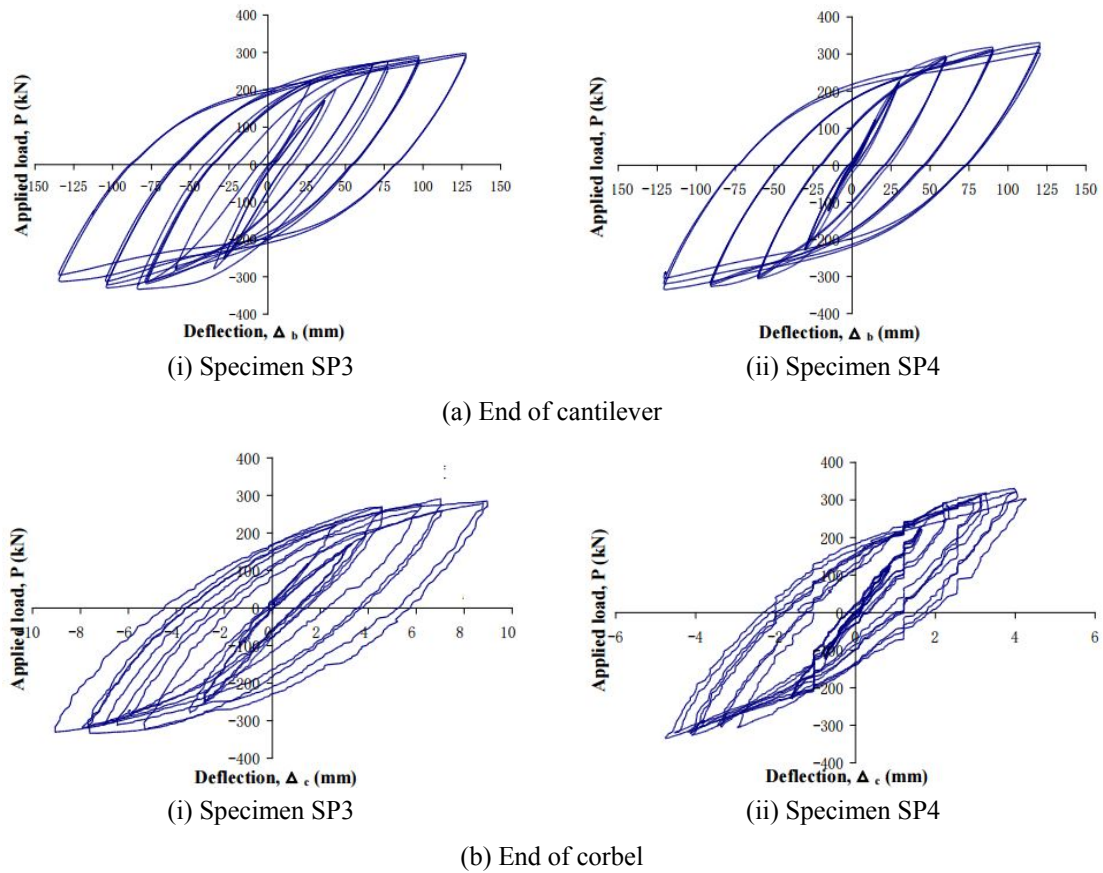


Fig. 11 Load-deflection curves

high connection ductility and energy absorbing capacities. As per an overall structural analysis on the Raffles City tower structure, the overall inter-floor drifting was controlled under $H/500$, where H is the storey height, under both wind and moderate earthquake. As per the push-over analysis on the tower structure, the demand on the maximum rotation of the connection under an extreme earthquake is 3.2 times of the first yield deformation. Thus, the deformation capacities of 4 times of the first yield deformation also fulfill the performance target of the Raffles City tower structures even under extreme earthquakes.

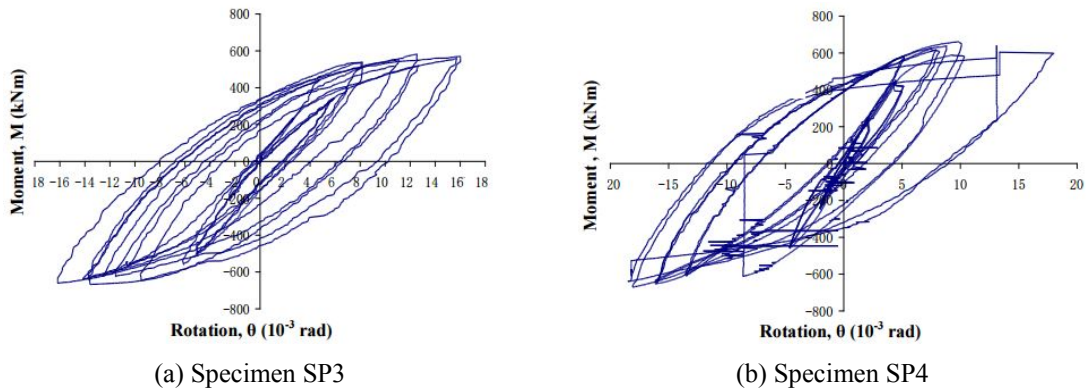
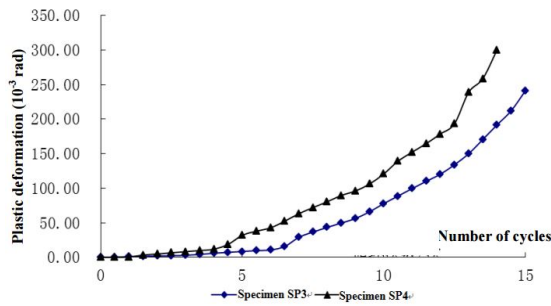
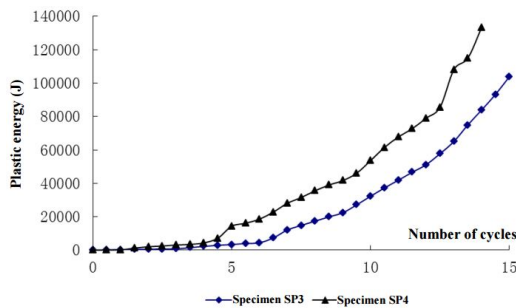


Fig. 12 Moment-rotation curves



(a) Cumulative plastic deformation



(b) Cumulative plastic energy

Fig. 13 Ductility and energy absorbing performance

Table 2 Summary of static tests and finite element simulation

		Applied load, P (kN)	Deflection, Δ (mm)	Applied moment, M (kNm)	Rotation, θ (rad)	Strain in top flange, ε_t ($\times 10^{-6}$)	Strain in bottom flange, ε_b ($\times 10^{-6}$)	Shear strain in web, ε_s ($\times 10^{-6}$)
SP 1	First yield	235.0	30.6	470.0	0.0042	1780	-1188	267
	Failure	321.0	98.3	642.0	0.0176	29635	-10684	2264
SP 2	First yield	211.1	25.6	422.2	0.0035	1782	-1047	316
	Failure	332.1	148.1	664.2	0.0178	33617	-6547	9352
FEM	First yield	220.3	29.3	450.2	0.0038	1780	-1134	304
	Failure	335.5	110.3	673.2	0.0175	30043	-8653	6345

Fig. 8 shows a typical failure mode of the composite connection. Obvious concrete cracking is initially observed near the outer surface of the corbel connection region, and crushing of concrete material and local buckling of longitudinal reinforcement are observed after multiple cycles of applied loads. While these local concrete cracking and crushing and reinforcement buckling under extreme deformation have quite limited impact on the load carrying capacity of the composite connections, despite some very slightly softening in the moment-deformation curves being observed during the test as shown in Figs. 11 and 12.

The cumulative plastic deformations of both Specimens SP3 and SP4 are 0.3 and 0.24 rad respectively as shown in Fig. 13, which are corresponding to 88 and 80 times the first yield rotation of the composite connections, see Table 2. This, again, demonstrates the high ductility and energy absorbing capacities of the corbel type composite connections.

7. Finite element modelling

To study the structural behaviour of the corbel type composite connection, a generalized nonlinear three-dimensional finite element model was set up using the commercial finite element package ANSYS 12.1 (2011). The meshes of the finite element model are shown in Fig. 14. In order to simplify the problem and save computational time, only half of the specimen was modelled.

7.1 Finite element mesh

Steel beams, corbels and steel tubular columns are modelled with eight-noded solid elements, Solid 45, while the concrete section is modelled with eight-noded solid elements, Solid 65, incorporating the steel reinforcement. More than 8 elements are arranged in the vertical direction of the steel corbel and beam, so that any flexural and shear action in the region can be captured accurately. The elements in the connection regions are locally refined so that local concrete crushing and splitting and steel yielding due to the interaction between the corbel as well as the CFT column and surrounding concrete can be captured. Reinforcement is also simulated with the same type of solid elements and assumed to be bonded perfectly to its surrounding concrete.

It is assumed that the steel beam, corbel and steel tubular column are bonded perfectly to the surrounding concrete material, so that there is no relative slippage between the steel and concrete portions of the corbel type composite connection.

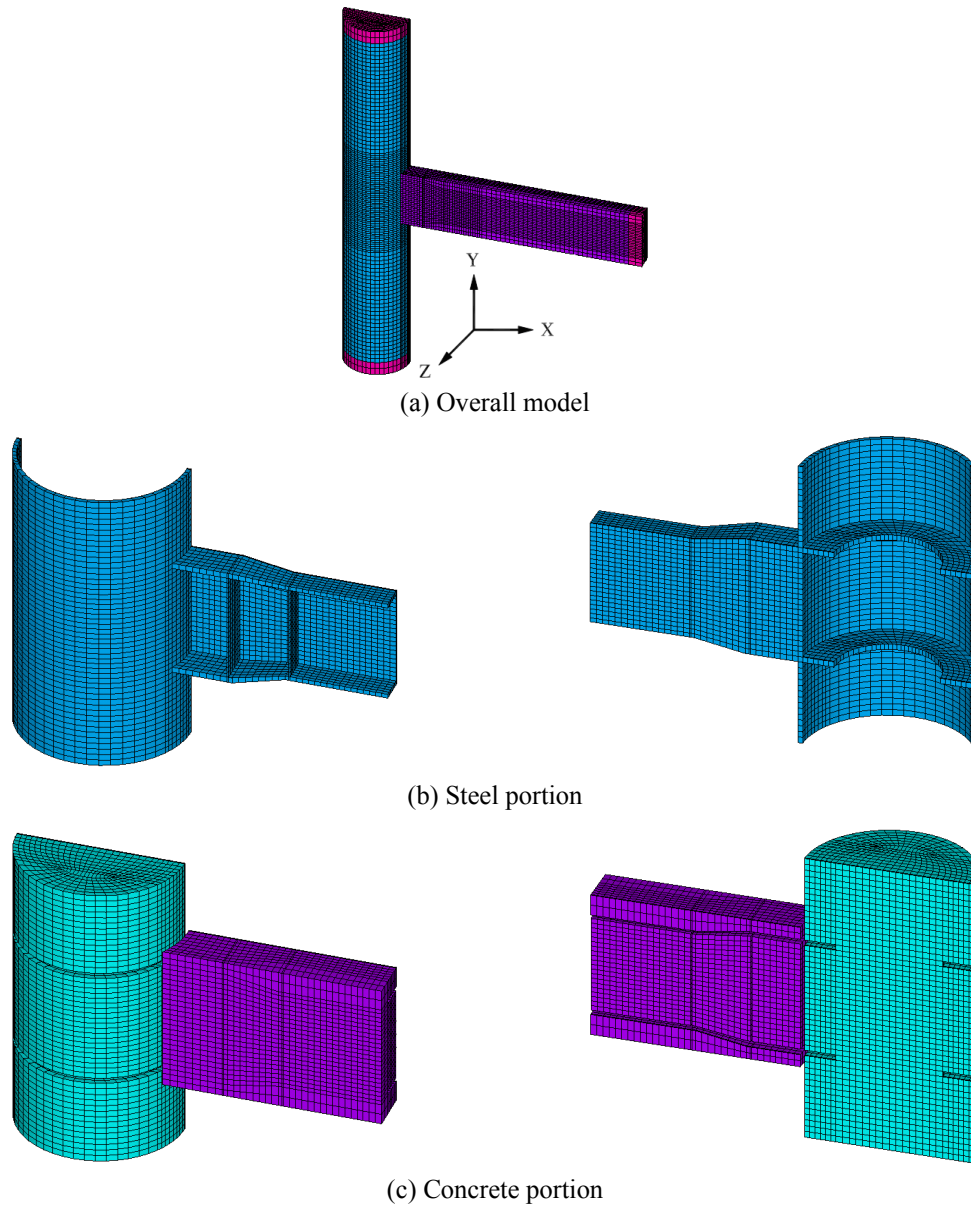


Fig. 14 Finite element model

7.2 Contact stiffness

Spring contact elements with large compressive stiffness and zero tensile stiffness are placed between the concrete section of the SRC beams and the steel tube of the CFT column. The value of the contact stiffness is assigned to be 20000 N/mm after a trial-and-error process in comparing the measured and the predicted load-slippage curves of a number of test specimens, and the value of contact stiffness are assumed to remain constant throughout the analysis.

7.3 Material models

A bi-linear stress-strain curve is adopted for the steel, as shown in Fig. 15(a). Failure of the steel sections and the shear connectors follows the von-Mises failure criteria whose failure surface is shown in the same figure.

A non-linear stress-strain curve is adopted in the material model of the concrete under uni-axial loading condition, as shown in Fig. 15(b). Crushing is included in the material model of concrete through the uni-axial definition of stress-strain curves for the concrete material under tri-axial compression. The failure surface of the concrete material follows the Drucker-Prager failure criteria (ANSYS 2011) as presented in Fig. 15(b). The friction angle of the concrete is taken as 67.5° for $p_t/p_c = 0.1$, where is p_t is the uni-axial tensile strength, and p_c is the cylinder strength.

Micro-cracking in the concrete slabs is simulated with a smeared cracking model. The tensile strength of concrete is taken as 10% of its compressive strength and assumed to reduce linearly from its peak value to zero at the tensile strain of 0.1% as shown in Fig. 15(b).

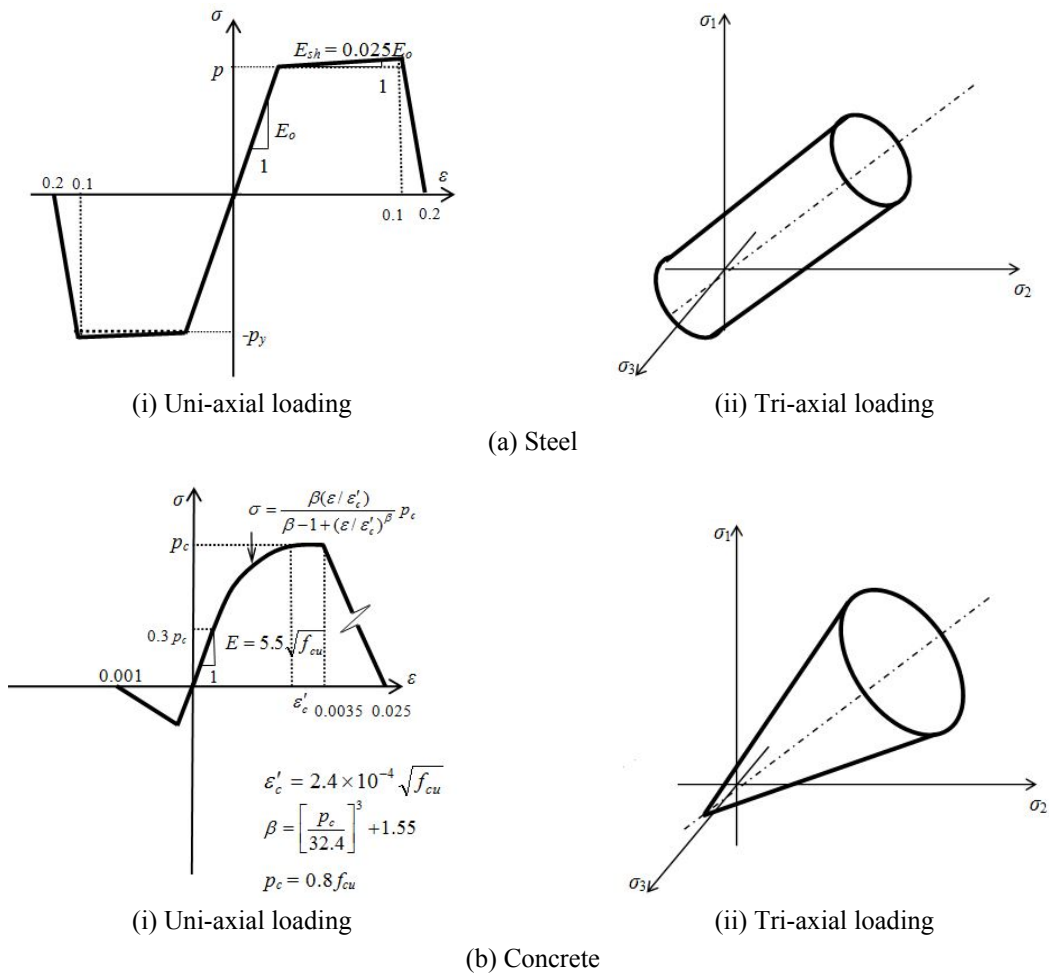


Fig. 15 Material models

7.4 Solution procedure

In this investigation, the solution procedure requires the full load to be applied in a series of small increments so that the solutions may follow the load-slippage closely. A value of 5% is recommended as the maximum plastic strain increment in each incremental load. In order to accurately model the large deformation at critical locations after steel yielding as well as local concrete crushing and splitting, both material and geometrical non-linearities were incorporated into the finite element model.

As this is a highly nonlinear problem, the solution is obtained through a number of equilibrium interactions for each load step. This is accomplished by an arch-length procedure in which the nodal displacements, the out-of-balance forces and the tangent stiffness matrix of the structure are updated after each equilibrium interaction. A force-based convergence criterion is adopted which requires the imbalance force is less than 0.5% of the average applied force in each equilibrium interaction.

8. Numerical results

8.1 Load carrying capacities

Table 2 summarizes the main results from both the monotonic physical tests and those from the numerical analyses. It is noted that the load carrying capacities predicted by the finite element analysis is 335.5 kN as compared with 321.0 and 332.1 kN for Specimens SP1 and SP2 respectively. The finite element analyses also give quite close results regarding the first yield loading as compared with the monotonic loading tests. This demonstrated that the proposed numerical model is able to give a properly accurate prediction to the load carrying capacities of the corbel type composite connection.

8.2 Load-deformation characteristics

Figs. 16(a) and (b) presents the load-deflection and load-strain curves as predicted by the finite element simulation for the composite connection. The results from the physical tests are plotted in the same diagram for the ease of comparison. The finite element simulation gives a quite close prediction of the load-deformation characteristics in the connection regions, which is demonstrated through the comparison of the load-deformation curves at the end of the connection corbel. While for the load-deformation curves at the end of the cantilever beams, the stiffness predicted by the finite element simulation is slightly higher than those by the physical monotonic loading tests. This is maybe because the possible slippage between the concrete and steel sections is not considered in the finite element simulation of the SRC beam, which leads to slight over-prediction for the beam stiffness.

8.3 Failure mode

Figs. 8(a) and (b) present the typical failure modes in both concrete and steel sections at the end of the physical monotonic tests. The failure mode predicted by the finite element analyses are shown in the same figures for direct comparison as well. It is noted that the concrete cracking near the outer side of the connection corbel is successful captured through the finite element modelling.

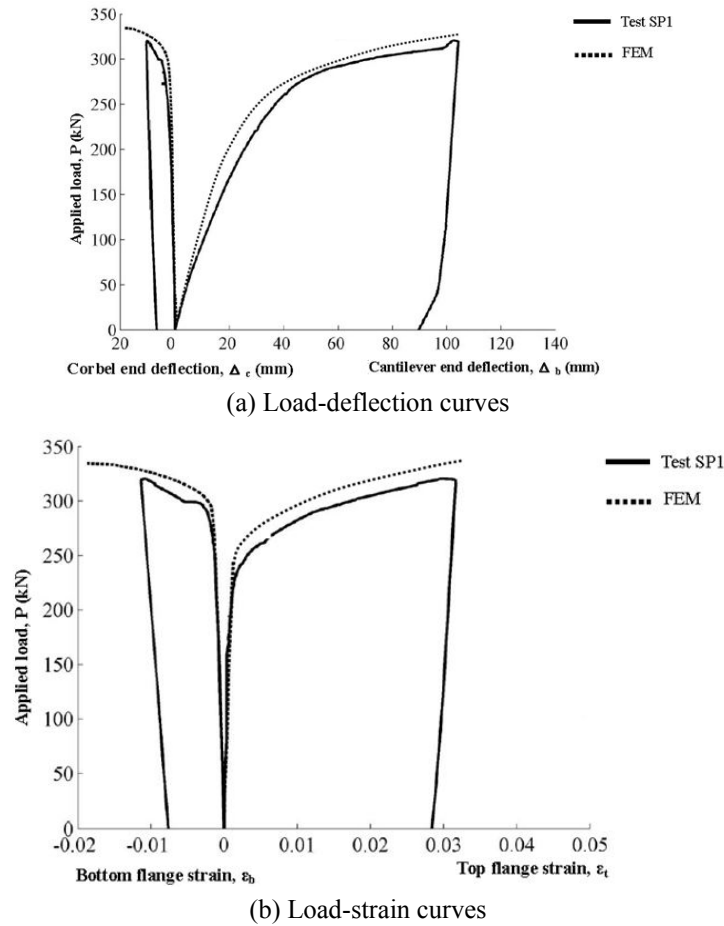


Fig. 16 Comparison between test and numerical results

The yielding of the steel in the connection region at extreme deformation is also well modelled as shown in Fig. 8(b), which demonstrates the accuracy of the proposed numerical model.

9. Conclusions

The studies present the results of experimental and numerical studies into the structural behaviour of the high performance corbel type composite connection. Through the physical tests under both monotonic and quasi-static cyclic loads, the load carrying capacities and deformation characteristics are studied carefully. A finite element model is also proposed was used for verification of the experimental results. Based on both the experimental and numerical studies, the following conclusions are drawn for the proposed corbel type composite connection:

- (1) By comparing the normalized moment-rotation curves with those defined in Eurocode 3, Part 1.8 (BSI 2005), it is observed that both full rigidity and full strength can be achieved through the proposed corbel type composite connection. The enlarged corbel is able to

effectively eliminate the potential loss of stiffness and strength at the interface between the SRC beam and the CFT column;

- (2) The deformation of the composite connections at failure is up to 4 times the deformation at the first yield, and the cumulative plastic deformations of the proposed composite connection is 80 to 88 times that at first yield, which demonstrate the ductility and good structural performance under the seismic action; and
- (3) The proposed finite element model is proved to be accurate to predict the structural behavior of the composite connection under both elastic and extreme deformation stages, and is readily to be extended to study the structural behaviour of composite connections with similar configurations but different dimensions.

With the booming in the construction industry in Asia in the past decades, more and more mega high-rise composite buildings are being developed, which require a high level of connection rigidity and ductility to ensure the overall building stability and safety under extreme loads. The proposed corbel type composite connection is able to meet a high level of rigidity, strength and ductility to suit the current trend in the construction industry. Thus, structural engineers are encouraged to adopt the proposed corbel type composite connection in mega high-rise buildings to achieve an economical and highly buildable and architectural friendly engineering solution.

References

- Ahmed, B. and Nethercot, D.A. (1996), "Effect of high shear on the moment capacity of composite cruciform endplate connections", *J. Construct. Steel Res.*, **40**(2), 129-163.
- American Institute of Steel Construction (2005), ANSI/AISC 360-05: Specification for Structural Steel Buildings.
- ANSYS (2011), User's Manual Version 12.1, ANSYS.
- ASTM (2011), E2126-11: Standard Test Methods for Cyclic (Reversed) Load Test for Shear Resistance of Vertical Elements of the Lateral Force Resisting Systems for Buildings.
- British Standards Institution (BSI) (2004), Eurocode 4: Design of Composite Steel and Concrete Structures, Part 1.1: General Rules and Rules for Buildings, European Committee for Standardization.
- British Standards Institution (BSI) (2005), Eurocode 3: Design of Steel Structures, Part 1.8: Design of Joints, European Committee for Standardization.
- Brockenbrough, R.L. and Merritt, F.S. (2006), *Structural Steel Designer's Handbook*, American Institute of Steel Construction.
- Brown, N.D. and Anderson, D. (2001), "Structural properties of composite major axis end plate connections", *J. Construct. Steel Res.*, **57**(3), 327-349.
- China Academy of Building Research (CABR) (1997), Specification of Test Methods for Earthquake Resistant Building, CABR.
- Davison, J.B., Lam, D. and Nethercot, D.A. (1990), "Semi-rigid action of composite joints", *Struct. Eng.*, **68**(24), 489-499.
- Fang, L.X., Chan, S.L. and Wong, Y.L. (2000), "Numerical analysis of composite frames with partial shear-stud interaction by one element per member", *Eng. Struct.*, **22**(10), 1285-1300.
- Lawson, R.M. and Gibbons, C. (1995), *Moment Connections in Composite Construction: Interim Guidance for End-plate Connections*; The Steel Construction Institute.
- Li, T.Q., Nethercot, D.A. and Choo, B.S. (1996), "Behaviour of flush end-plate composite connections with unbalanced moment and variable shear/moment ratios. Part 1: Experimental behaviour", *J. Construct. Steel Res.*, **38**(2), 125-164.
- Nethercot, D.A. and Li, T.Q. (1995), "Design of semi-continuous composite frames", *Proceedings of*

- International Conference on Structural Stability and Design*, Sydney, Australia, October-November, pp. 277-282.
- Queiroz, G., Mata, L.A.C. and Franco, J.R.Q. (2005), "Analysis of composite connections in unbraced frames subjected to wind and gravity load", *J. Construct. Steel Res.*, **61**(8), 1075-1093.
- The Steel Construction Institute (SCI) & The British Constructional Steelwork Association Limited (BCSA) (2002), *Joints in Steel Construction*, the Steel Construction Institute.
- Vasdravellis, G., Valente, M. and Castiglioni, C.A. (2009a), "Behaviour of exterior partial-strength composite beam-to-column connections: Experimental study and numerical simulations", *J. Construct. Steel Res.*, **65**(1), 23-35.
- Vasdravellis, G., Valente, M. and Castiglioni, C.A. (2009b), "Dynamic response of composite frames with different shear connection degree", *J. Construct. Steel Res.*, **65**(10-11), 2050-2061.
- Wang, A.J. (2010), "A study on composite end-plate connections with flexible tensile reinforcements and shear connectors", *Can. J. Civil Eng.*, **37**(11), 1437-1450.
- Wang, A.J. (2011), "Studies on composite joints under gravity and lateral loads", *Australian J. Struct. Eng.*, **12**(1), 69-85.
- Wang, A.J. (2012), "A study on semi-continuous composite beams with realistic modelling of end-plate connections", *Australian J. Struct. Eng.*, **13**(3), 259-277.
- Xiao, Y., Choo, B.S. and Nethercot, D.A. (1994), "Composite connections in steel and concrete. Part 1: Experimental behaviour of composite beam-column connections", *J. Construct. Steel Res.*, **31**(1), 3-30.

BU